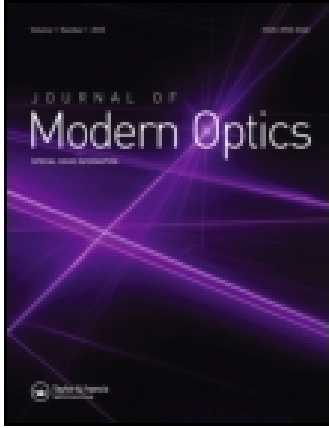


This article was downloaded by: [Hefei Institutes of Physical Science]

On: 21 April 2015, At: 19:14

Publisher: Taylor & Francis

Informa Ltd Registered in England and Wales Registered Number: 1072954 Registered office: Mortimer House, 37-41 Mortimer Street, London W1T 3JH, UK



## Journal of Modern Optics

Publication details, including instructions for authors and subscription information:

<http://www.tandfonline.com/loi/tmop20>

### Radiation forces of highly focused radially polarized hollow sinh-Gaussian beams on a Rayleigh metallic particle

Zhou Zhang<sup>ab</sup>, Hua-Feng Xu<sup>bc</sup>, Jun Qu<sup>d</sup> & Wei Huang<sup>abc</sup>

<sup>a</sup> Institute of Physics and Materials Science, Anhui University, Hefei, China

<sup>b</sup> Laboratory of Atmospheric Physico-Chemistry, Anhui Institute of Optics & Fine Mechanics, Chinese Academy of Sciences, Hefei, China

<sup>c</sup> School of Environmental Science & Optoelectronic Technology, University of Science and Technology of China, Hefei, China

<sup>d</sup> Department of Physics, Anhui Normal University, Wuhu, China

Published online: 03 Feb 2015.



[Click for updates](#)

To cite this article: Zhou Zhang, Hua-Feng Xu, Jun Qu & Wei Huang (2015) Radiation forces of highly focused radially polarized hollow sinh-Gaussian beams on a Rayleigh metallic particle, *Journal of Modern Optics*, 62:9, 754-760, DOI: [10.1080/09500340.2015.1005188](https://doi.org/10.1080/09500340.2015.1005188)

To link to this article: <http://dx.doi.org/10.1080/09500340.2015.1005188>

PLEASE SCROLL DOWN FOR ARTICLE

Taylor & Francis makes every effort to ensure the accuracy of all the information (the "Content") contained in the publications on our platform. However, Taylor & Francis, our agents, and our licensors make no representations or warranties whatsoever as to the accuracy, completeness, or suitability for any purpose of the Content. Any opinions and views expressed in this publication are the opinions and views of the authors, and are not the views of or endorsed by Taylor & Francis. The accuracy of the Content should not be relied upon and should be independently verified with primary sources of information. Taylor and Francis shall not be liable for any losses, actions, claims, proceedings, demands, costs, expenses, damages, and other liabilities whatsoever or howsoever caused arising directly or indirectly in connection with, in relation to or arising out of the use of the Content.

This article may be used for research, teaching, and private study purposes. Any substantial or systematic reproduction, redistribution, reselling, loan, sub-licensing, systematic supply, or distribution in any form to anyone is expressly forbidden. Terms & Conditions of access and use can be found at <http://www.tandfonline.com/page/terms-and-conditions>

## Radiation forces of highly focused radially polarized hollow sinh-Gaussian beams on a Rayleigh metallic particle

Zhou Zhang<sup>a,b</sup>, Hua-Feng Xu<sup>b,c</sup>, Jun Qu<sup>d\*</sup> and Wei Huang<sup>a,b,c\*</sup>

<sup>a</sup>*Institute of Physics and Materials Science, Anhui University, Hefei, China;* <sup>b</sup>*Laboratory of Atmospheric Physico-Chemistry, Anhui Institute of Optics & Fine Mechanics, Chinese Academy of Sciences, Hefei, China;* <sup>c</sup>*School of Environmental Science & Optoelectronic Technology, University of Science and Technology of China, Hefei, China;* <sup>d</sup>*Department of Physics, Anhui Normal University, Wuhu, China*

(Received 24 November 2014; accepted 17 December 2014)

Based on the vector diffraction theory, the tight focusing properties of radially polarized hollow sinh-Gaussian (HsG) beams are theoretically studied. It is found that the radially polarized HsG beams can form a longitudinally polarized sub-wavelength focal spot. Moreover, the radiation forces acting on a Rayleigh metallic particle are calculated for the case where the radially polarized HsG beams are applied. Compared with the use of conventional Gaussian beams, the high-order radially polarized HsG beams can largely enhance the radial trap stiffness and broaden the axial trap distance. The influence of the beam order  $m$  on the focusing properties and trap stiffness is investigated in detail.

**Keywords:** focusing properties; polarization; radiation forces; trap stiffness

### 1. Introduction

Optical tweezers use the radiation forces exerted by a highly focused beam to trap and manipulate objects ranging in size from tens of nanometres to tens of micrometres. Since it was invented in 1986 by Ashkin and his co-workers [1], optical trapping and manipulation have become a hot topic in scientific community. Now, optical tweezers have been widely used in various areas of science, particularly in physics, chemistry and biophysical studies, for example, trapping and manipulating microscopic particles [2–11], manipulation of a single electron spin [12], trapping a gold nanopillar [13], controlling or trapping single aerosol [14,15], stretching DNA [16], trapping red blood cells in living animals [17] and so on. Thus, optical tweezers have been developed into one of the most promising tools in microscopic research [18].

As we all know, polarization is one of the most important and intrinsic properties of light. This vector nature of light and its interactions with matter make many optical devices and optical system designs possible [19]. In general, the beams can be classified into two categories in terms of the state of polarization. The first type is spatially homogeneous polarized beams. This type of polarized beams, including linearly, circularly and elliptically polarized beams, is most familiar to the optical community. The second type is spatially inhomogeneous polarized beams, such as cylindrical vector (CV) beams. In recent years, there has been a rapid increase of the number of publications on the CV beams

[3–5,19–23], due to their interesting properties and potential applications. It has been found that the highly focused radially polarized beams can produce a tighter spot with an extremely strong longitudinal component near the focus. Such a strong longitudinal component can provide a large gradient force, while it does not contribute to Poynting vector along the propagation direction and thus does not create axial scattering and absorption forces [3]. Due to these special features, using the radially polarized beams can largely improve the performance of an optical trap system compared with the usage of linearly polarized beams, especially for trapping metallic particles [3].

Until now, the tight focusing properties and the trapping characteristics of different beams, such as CV beams [3–5], series of Gaussian beams [24,25], Bessel beams [26], full Poincaré beams [27,28], coherent and partially coherent beams [6,29], and vortex beams [30,31] have been studied. It has been found that the focusing properties and the trapping characteristics of the laser beams are mainly related to the beam's characteristic, such as beam's profile, polarization and coherence. Recently, the dark hollow beams with zero central intensity have attracted a lot of attention due to their special features and potential applications in atom guiding, focusing and trapping [32–39]. In 2012, Sun et al. introduced a new mathematical model of dark hollow beams, described as hollow sinh-Gaussian (HsG) beams which can be considered as the superposition of a series of eccentric Gaussian

\*Corresponding authors. Email: [qujun70@mail.ahnu.edu.cn](mailto:qujun70@mail.ahnu.edu.cn) (J. Qu), [huangwei6@ustc.edu.cn](mailto:huangwei6@ustc.edu.cn) (W. Huang)

beam [38]. It is shown that the intensity profile of HsG beams at the original plane can be characterized by a single bright ring whose size is determined by the beam order. The experimental generation of such HsG beams has not been reported yet, but it may be realized using a liquid crystal spatial light modulator [40–42]. In theory, Lin et al. have investigated the focusing properties of the radially polarized HsG beams based on the Richards–Wolf theory [39]. However, as far as we know, there are no papers dealing with the radiation forces produced by the highly focused radially polarized HsG beams on the Rayleigh metallic particles. However, this topic seems important since the highly focused radially polarized HsG beams can form a longitudinally polarized sub-wavelength focal spot, which could be of great importance for the laser trapping and manipulation. In this paper, our main purpose is to study the radiation forces produced by the highly focused radially polarized HsG beams acting upon a Rayleigh metallic particle. The influence of the beam order on the focusing properties and trap stiffness is investigated in detail. Our research can improve the understanding of the focusing properties and trapping characteristics for the highly focused radially polarized HsG beams, which will be useful for experimental trapping by means of optical tweezers.

## 2. Formulas and focusing properties of any order radially polarized HsG beams

The electric field of HsG incident beams at the original plane can be defined as follows [38]:

$$E_m(r) = \sinh^m\left(\frac{r}{w_0}\right) \exp\left(-\frac{r^2}{w_0^2}\right), \quad (m = 0, 1, 2, 3, \dots) \quad (1)$$

where  $m$  and  $w_0$  is the beam order and the beam waist of the HsG beams, respectively. Obviously, for the case of  $m = 0$ , Equation (1) reduces to the expression for the electric field of a conventional Gaussian beam. When  $m \geq 1$ , the HsG beams show a doughnut-shaped intensity distribution at the original plane, and its dark hollow area will increase gradually with the increases of the beam order  $m$  and beam waist  $w_0$ , respectively [38,39]. For typical objective lenses that obey the sine condition, the ray projection function is given by  $r = f \sin \theta$ . Thus, the electric field of the HsG beams at a pupil can be rewritten as [39]:

$$E_m(\theta) = \sinh^m\left(\frac{\sin \theta}{\sigma_0}\right) \exp\left(-\frac{\sin^2(\theta)}{\sigma_0^2}\right) \quad (2)$$

where  $\sigma_0 = w_0/f$  is the relative beam size. According to the Richards–wolf theory [43], the electric field components in the vicinity of the focus of radially polarized HsG beams can be obtained as follows:

$$\mathbf{E}_r(\mathbf{r}, \mathbf{z}) = A \int_0^\alpha \cos^{1/2}\theta \sin(2\theta) E_m(\theta) J_1(k_1 r \sin \theta) \exp(ik_1 z \cos \theta) d\theta \quad (3)$$

$$\mathbf{E}_z(\mathbf{r}, \mathbf{z}) = -2iA \int_0^\alpha \cos^{1/2}\theta \sin^2 \theta E_m(\theta) J_0(k_1 r \sin \theta) \exp(ik_1 z \cos \theta) d\theta \quad (4)$$

where the azimuthal component of the electric field is zero everywhere in the diffraction field. An azimuthally polarized magnetic field can be produced, this field can be found from Maxwell's equations, that is [44],

$$\mathbf{H}_\phi(\mathbf{r}, \mathbf{z}) = \frac{2An_1}{\mu_0 c} \int_0^\alpha \cos^{1/2}\theta \sin \theta E_m(\theta) J_1(k_1 r \sin \theta) \exp(ik_1 z \cos \theta) d\theta \quad (5)$$

in Equations (2)–(5),  $\alpha = \arcsin(NA/n_1)$  which represents the maximal value of the convergence angle  $\theta$ ,  $n_1$  is the refractive index of the immersion liquid.  $A = E_0 \pi f n_1 / \lambda$  is a constant with  $f$  being the focal length,  $E_0$  is the amplitude of electric field which is related to the power of the incident beam,  $k_1 = 2\pi n_1 / \lambda$  is the wave number. Figure 1 shows the intensity distribution of the radially polarized HsG beams with three different values of beam order  $m$  at the original plane and the schematic of the tight focused system, respectively.

In the following calculations, the numerical aperture of the focusing lens is chosen as  $NA = 0.95n_1$ , the immersion liquid is water with a refractive index of  $n_1 = 1.332$ , the laser wavelength  $\lambda$  is  $1.047 \mu\text{m}$ , the relative beam size  $\sigma_0 = 0.5$  and the power of the incident beam is 100 mW. Figure 2 shows the focal intensity distribution of the radially polarized HsG beams with three different values of beam order  $m$ , respectively. From Figure 2(a1)–(c1), it is shown that the focal spot size of the conventional Gaussian beams (i.e.  $m = 0$ ) is much larger than that of the HsG beams. As the increase of  $m$ , the focal spot size gets narrower and the depth of focus (DOF) simultaneously becomes longer for the HsG beams. From Figure 2(a2)–(c2), one can find that the total focused field is determined by radial and longitudinal components. The radial component shows a dark hollow shape while the longitudinal component has a sharp peak profile at the focal plane. Furthermore, with  $m$  changing from 0 to 8, the radial component can be largely suppressed, while the longitudinal component can be greatly enhanced. Finally, the longitudinal component will become dominant in the total field. Thus, the longitudinally polarized sub-wavelength focal spot can be generated.

To further study the influence of beam order  $m$  on the focusing properties of radially polarized HsG beams, Figure 3 shows the dependence of the focal spot (red

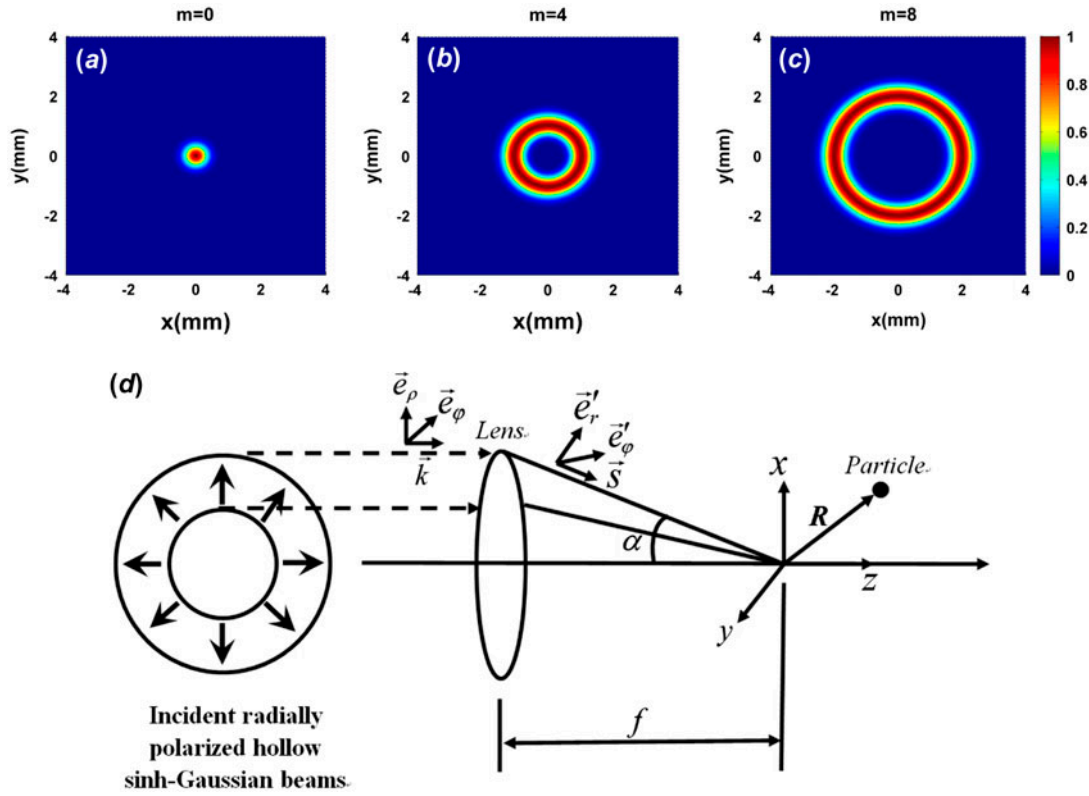


Figure 1. (a)–(c) Contour plots for intensity distribution at the original plane for  $m = 0$ ,  $m = 4$  and  $m = 8$ , respectively; (d) the scheme of the tight focusing system. (The colour version of this figure is included in the online version of the journal.)

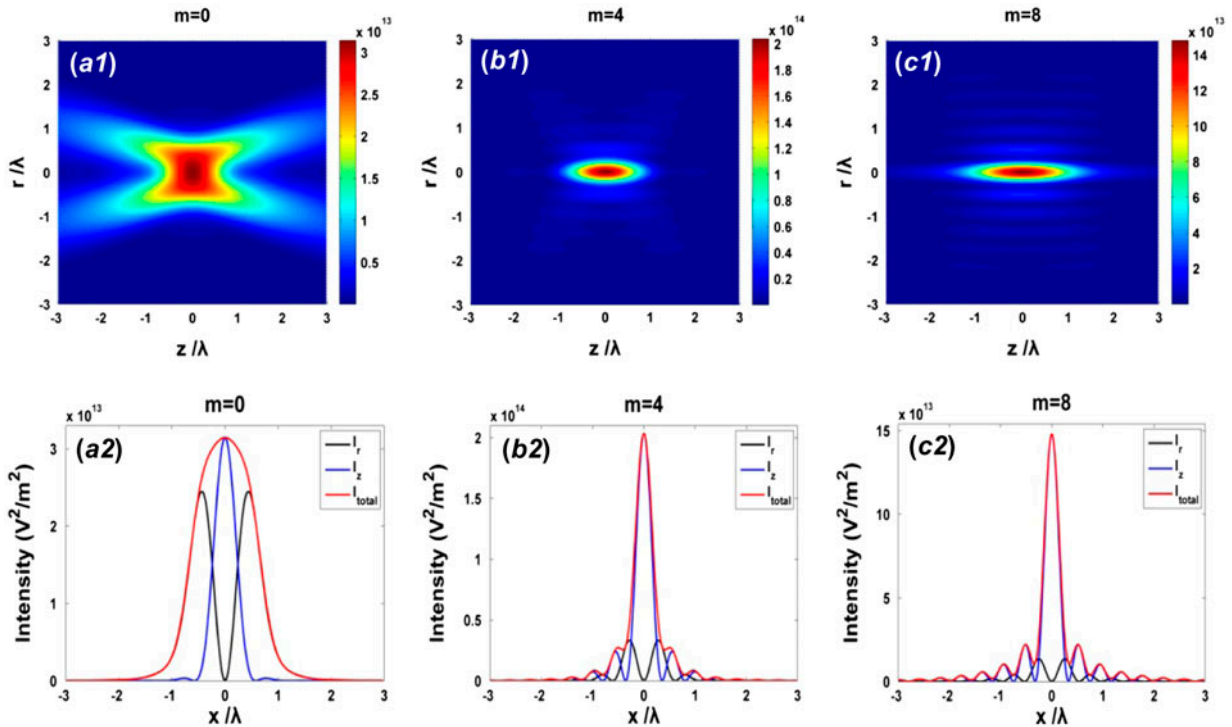


Figure 2. (a1)–(c1) Contour plots for intensity distribution in the  $r$ - $z$  plane; (a2)–(c2) the cross-section intensity profiles of radial, longitudinal and the total field components for  $m = 0$ ,  $m = 4$  and  $m = 8$ , respectively. (The colour version of this figure is included in the online version of the journal.)

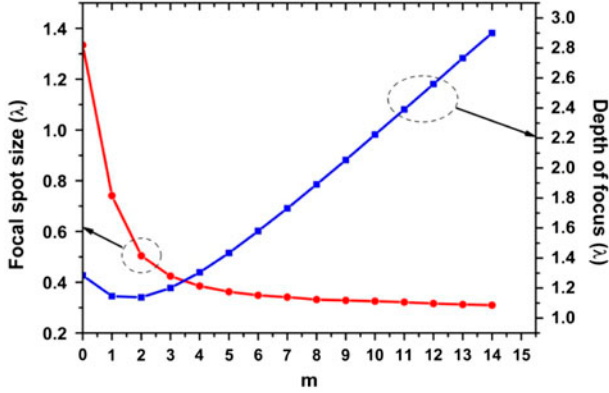


Figure 3. Focal spot size and depth of the focus as a function of the beam order  $m$ . The other parameters are the same as Figure 2. (The colour version of this figure is included in the online version of the journal.)

line) and the DOF (blue line) on the beam order, respectively. One can find that with increase of  $m$ , the focal spot size decreases rapidly at first (about  $0 \leq m \leq 3$ ), while decreases more slowly and gradually approaches the minimum value (about  $0.3\lambda$ ) with the further increasing of  $m$ . For the DOF, as the  $m$  increases, it decreases a little at the beginning (about  $0 \leq m \leq 2$ ), and then, it turns to increase steadily.

### 3. Radiation forces produced by highly focused radially polarized HsG beams on a Rayleigh metallic particle

For Rayleigh metallic particles, the radius  $a$  of the particle is much smaller than the wavelength of the beam (generally  $a \leq \lambda/20$ ), the dipole approximation can be used to calculate the radiation forces [3,45]. The total optical force acting on a metallic particle can be divided into three parts: the gradient force  $F_{\text{grad}}$ , the absorption

force  $F_a$  and the scattering force  $F_s$ . The gradient forces can pull the gold particle towards the centre of the focus while the absorption and scattering forces tend to push the particle out of focus and destabilize the optical trap. Thus, for a stable trapping, the gradient force should overcome the absorption and scattering forces. According to the Rayleigh scattering theory, these forces can be expressed as follows:

$$F_{\text{grad}}(\mathbf{r}, z) = \frac{\text{Re}(\gamma)\xi_0 \nabla I(\mathbf{r}, z)}{4} \quad (6)$$

$$F_a = n_1 \langle \mathbf{S} \rangle C_{\text{abs}}/c \quad (7)$$

$$F_s = n_1 \langle \mathbf{S} \rangle C_{\text{scat}}/c \quad (8)$$

where  $\gamma = 4\pi a^3 \xi_1 (\xi_2 - \xi_1) / (\xi_2 + 2\xi_1)$  is the polarizability of the metallic particle with  $\xi_2$  and  $\xi_1$  being the relative permittivity of the metallic particle and the ambient, respectively. In our calculations, we assume that the radius of the gold particle is 19.1 nm, and relative permittivity of the particle is  $\xi_2 = -54 + 5.9i$  [3].  $C_{\text{scat}} = k^4 |\gamma|^2 / 6\pi$  and  $C_{\text{abs}} = kn_1 \text{Im}(\gamma) / \xi_1$  are the scattering and absorption cross sections of the particle, respectively.  $\langle \mathbf{S} \rangle$  is the time-averaged Poynting vector of the highly focused radially polarized HsG beams, which is given as:

$$\langle \mathbf{S} \rangle = \frac{1}{2} \left[ \text{Re}(\mathbf{E}_r \mathbf{H}_\varphi^*) \vec{e}_z - \text{Re}(\mathbf{E}_z \mathbf{H}_\varphi^*) \vec{e}_r \right] \quad (9)$$

Figure 4 shows the total transverse trapping forces  $F_t = F_{g,t} + F_{s,t} + F_{a,t}$  acting on a Rayleigh metallic particle for three different values of beam order  $m$  in the focal plane and at the off-focus distance of  $z = \lambda$ , respectively. From Figure 4(a), one can find that the particle can be trapped at the focus, and the HsG beams (i.e.  $m = 4, 8$ ) can provide a much larger total transverse trapping force compared with that of the conventional

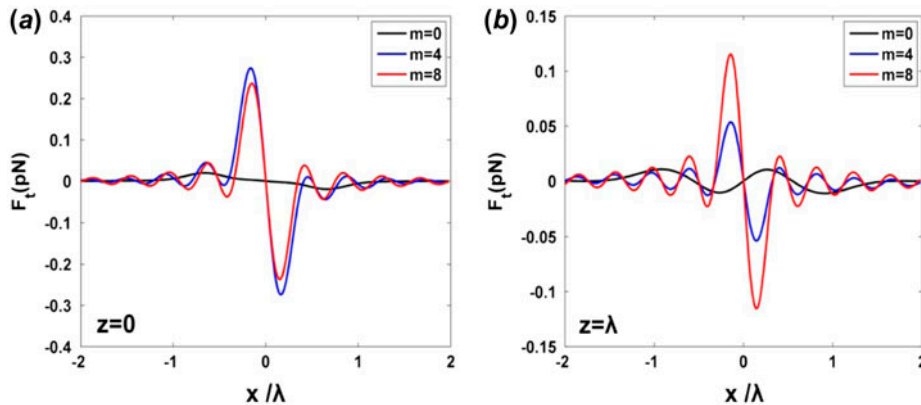


Figure 4. The total transverse trapping force  $F_t$  acting on a Rayleigh metallic particle along the  $x$ -axis for three different values of beam order  $m$ , (a) in the focal plane, (b) at the off-focus distance of  $z = \lambda$ . The other beam parameters are the same as Figure 2. (The colour version of this figure is included in the online version of the journal.)

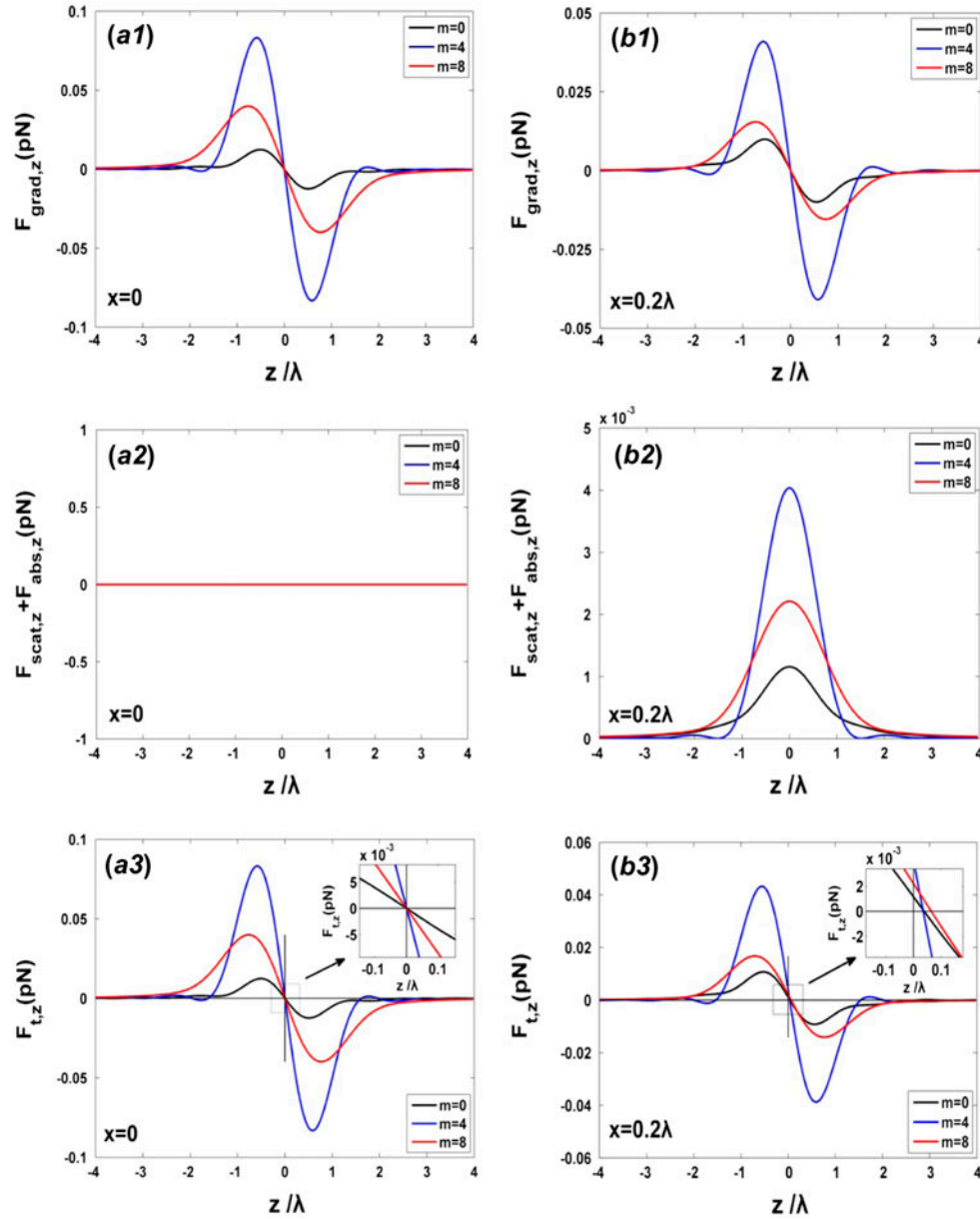


Figure 5. The longitudinal gradient force ((a1) and (b1)), the sum of the longitudinal absorption and scattering forces ((a2) and (b2)), and the total longitudinal trapping force ((a3) and (b3)) for three different values of  $m$  at two different off-axis distances of  $x = 0$  and  $x = 0.2\lambda$ . The other beam parameters are the same as Figure 2. (The colour version of this figure is included in the online version of the journal.)

Gaussian beams (i.e.  $m = 0$ ). Moreover, one can also find from Figure 4(b) that the conventional Gaussian beams cannot trap the particle at the off-focus distance of  $z = \lambda$  anymore, whereas the HsG beams can still trap the particle stably. This phenomenon means that we can improve the transverse trapping stability and increase the axial trap range using high-order radially polarized HsG beams.

Figure 5 shows the longitudinal gradient force  $F_{\text{grad},z}$ , the sum of the longitudinal absorption and scattering forces ( $F_{\text{abs},z} + F_{\text{scat},z}$ ) and the total longitudinal trapping

force  $F_{t,z} = (F_{\text{grad},z} + F_{\text{abs},z} + F_{\text{scat},z})$  acting on a Rayleigh metallic particle for two cases of on the  $z$ -axis and at the off-axis distances of  $x = 0.2\lambda$ , respectively. From Figure 5(a), one can see that the sum of the scattering and absorption forces is essentially equal to zero along the  $z$ -axis due to the vanishing of axial Poynting vector under tight focusing conditions, and thus the particle can be trapped at the focus along the longitudinal direction. For the conventional Gaussian beams (i.e.  $m = 0$ ), the longitudinal gradient force is much smaller than that of the HsG beams (i.e.  $m = 4, 8$ ). For the HsG

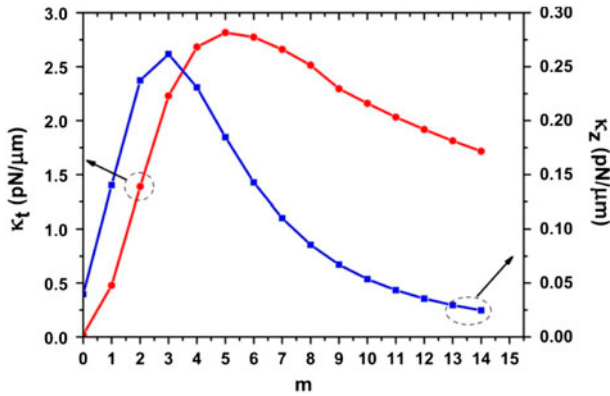


Figure 6. Dependence of the transverse and longitudinal trap stiffness on the beam order  $m$  of the radially polarized HsG beams at the focal point, respectively. The other beam parameters are the same as Figure 2. (The colour version of this figure is included in the online version of the journal.)

beams, with  $m$  increasing from 4 to 8, the longitudinal trap range can be broadened, even though the longitudinal gradient force will be decreased. Besides, as shown in Figure 5(b), when the particle locates at the off-axis position of  $x = 0.2\lambda$ , it will suffer strong scattering and absorption forces, while the gradient force is still much larger than the scattering and absorption forces. Thus, an extremely small shift of the trap equilibrium will appear along the propagation direction (see Figure 5(b3)), for example, the trap equilibrium position is  $z_{\text{equ}} = 0.065\lambda$  for the case of  $m = 8$ .

Besides the optical trapping forces, the magnitude of trap stiffness can reflect the trapping stability directly. Generally, the transverse and longitudinal trap stiffness can be expressed as [46]  $\kappa_t = |\partial F_t / \partial x|_{x_{\text{equ}}}$  and  $\kappa_z = |\partial F_t / \partial z|_{z_{\text{equ}}}$ , respectively. Figure 6 shows the dependence of the transverse (red line) and longitudinal (blue line) trap stiffness on the beam order  $m$  at the focal spot, separately. One can find from Figure 6 that with the increase of  $m$ , both of the transverse and longitudinal trap stiffness of the radially polarized HsG beams will increase firstly and then decrease. Therefore, choosing a suitable value of the beam order  $m$  is a feasible method for improving the trapping stability for the radially polarized HsG beams.

#### 4. Discussions on trapping stability

In order to stably trap and manipulate the gold particles, the longitudinal gradient force must be large enough to overcome the forward scattering/absorption forces, that is,  $R = |\mathbf{F}_{\text{grad},z}| / |\mathbf{F}_{\text{scat},z} + \mathbf{F}_{\text{abs},z}| \geq 1$ , where the ratio  $R$  is called the stability criterion. Obviously, we can find from Figure 5 that the magnitude of the gradient force is considerable larger than the sum of absorption and scattering forces for the radially polarized HsG beams, and thus

this stability criterion can be easily satisfied. In addition, for a Rayleigh metallic particle, the disturbance from the Brownian motion due to the thermal fluctuation from the surrounding medium will strongly affect the trapping stability. Thus, the potential well generated by the gradient force should be deep enough to overcome its kinetic energy in Brownian motion, that is,  $R_{\text{Thermal}} = e^{-U_{\text{max}}/K_B T} \ll 1$ , where the potential depth is given by [1]  $U_{\text{max}} = \xi_0 \text{Re}(\gamma) |\mathbf{E}|_{\text{max}}^2 / 2$ ,  $K_B$  is the Boltzmann constant. Assuming a temperature of 300 K,  $R_{\text{Thermal}}$  for the situations considered above is calculated to be  $5.7 \times 10^{-17}$  ( $m = 4$ ) and  $1.6 \times 10^{-12}$  ( $m = 8$ ) approximately. Obviously, the criterion  $R_{\text{Thermal}}$  can also be easily satisfied for the radially polarized HsG beams.

#### 5. Conclusions

In summary, we have theoretically investigated the focusing properties and the radiation forces acting on a Rayleigh metallic particle produced by the highly focused radially polarized HsG beams. It has been found that the radially polarized HsG beams can generate a longitudinally polarized sub-wavelength focal spot. More importantly, this feature can be greatly helpful for trapping Rayleigh metallic particles. The influence of the beam order  $m$  on the focusing properties, radiation forces and trap stiffness is investigated in detail. Our results have shown that we can choose a suitable beam order of the radially polarized HsG beams to largely enhance the transverse trapping stability and broaden the longitudinal trap range compared with the usage of the conventional Gaussian beams. Finally, the trapping stability is also analysed. Our results presented here would be useful for the experimental particle trapping.

#### Acknowledgements

This work is supported by the National Natural Science Foundation of China (NSFC) [grant number 21133008 and 11374015]. Acknowledgement is also made to the Thousand Youth Talents Plan, and ‘‘Interdisciplinary and Cooperative Team’’ of CAS.

#### Funding

This work is supported by the National Natural Science Foundation of China (NSFC) [grant number 21133008 and 11374015].

#### References

- [1] Ashkin, A.; Dziedzic, J.; Bjorkholm, J.; Chu, S. *Opt. Lett.* **1986**, *11*, 288–290.
- [2] Svoboda, K.; Block, S.M. *Opt. Lett.* **1994**, *19*, 930–932.
- [3] Zhan, Q. *Opt. Express* **2004**, *12*, 3377–3382.
- [4] Zhan, Q. *J. Opt. A: Pure Appl. Opt.* **2003**, *5*, 229.
- [5] Liu, Z.; Zhao, D. *Appl. Opt.* **2013**, *52*, 1310–1316.

- [6] Zhao, C.; Cai, Y. *Opt. Lett.* **2011**, *36*, 2251–2253.
- [7] Peng, F.; Yao, B.; Yan, S.; Zhao, W.; Lei, M. *J. Opt. Soc. Am. B*: **2009**, *26*, 2242–2247.
- [8] Zhang, Y.; Ding, B.; Suyama, T. *Phys. Rev. A* **2010**, *81*, 023831.
- [9] Mohanty, S.; Verma, R.; Gupta, P. *Appl. Phys. B* **2007**, *87*, 211–215.
- [10] Yan, S.; Yao, B. *Phys. Rev. A* **2007**, *76*, 053836.
- [11] Gahagan, K.; Swartzlander, G. *J. Opt. Soc. Am. B*: **1998**, *15*, 524–534.
- [12] Geiselmann, M.; Juan, M.L.; Renger, J.; Say, J.M.; Brown, L.J.; De Abajo, F.J.G.; Koppens, F.; Quidant, R. *Nat. Nanotechnol.* **2013**, *8*, 175–179.
- [13] Wang, K.; Crozier, K.B. *ChemPhysChem*. **2012**, *13*, 2639–2648.
- [14] Hopkins, R.J.; Mitchem, L.; Ward, A.D.; Reid, J.P. *Phys. Chem. Chem. Phys.* **2004**, *6*, 4924–4927.
- [15] Dear, R.D.; Burnham, D.R.; Summers, M.D.; McGloin, D.; Ritchie, G.A. *Phys. Chem. Chem. Phys.* **2012**, *14*, 15826–15831.
- [16] Wang, M.D.; Yin, H.; Landick, R.; Gelles, J.; Block, S.M. *Biophys. J.* **1997**, *72*, 1335–1346.
- [17] Zhong, M.; Wei, X.; Zhou, J.; Wang, Z.; Li, Y. *Nat. Commun.* **2013**, *4*, 1768.
- [18] Grier, D.G. *Nature* **2003**, *424*, 810–816.
- [19] Zhan, Q. *Adv. Opt. Photonics* **2009**, *1*, 1–57.
- [20] Zhan, Q.; Leger, J. *Opt. Express* **2002**, *10*, 324–331.
- [21] Chen, W.; Zhan, Q. *Opt. Commun.* **2006**, *265*, 411–417.
- [22] Wang, X.; Ding, J.; Qin, J.; Chen, J.; Fan, Y.; Wang, H. *Opt. Commun.* **2009**, *282*, 3421–3425.
- [23] Guo, L.; Tang, Z.; Liang, C.; Tan, Z. *Opt. Laser Technol.* **2011**, *43*, 895–898.
- [24] Meyrath, T.; Schreck, F.; Hanssen, J.; Chuu, C.; Raizen, M. *Opt. Express* **2005**, *13*, 2843–2851.
- [25] Bhattacharya, M.; Meystre, P. *Phys. Rev. Lett.* **2007**, *99*, 153603.
- [26] Garcés-Chávez, V.; Roskey, D.; Summers, M.; Melville, H.; McGloin, D.; Wright, E.; Dholakia, K. *Appl. Phys. Lett.* **2004**, *85*, 4001–4003.
- [27] Beckley, A.M.; Brown, T.G.; Alonso, M.A. *Opt. Express* **2010**, *18*, 10777–10785.
- [28] Wang, L. *Opt. Express* **2012**, *20*, 20814–20826.
- [29] Wang, L.; Zhao, C.; Wang, L.; Lu, X.; Zhu, S. *Opt. Lett.* **2007**, *32*, 1393–1395.
- [30] Shu, J.; Chen, Z.; Pu, J. *J. Opt. Soc. Am. A*: **2013**, *30*, 916–922.
- [31] Gahagan, K.; Swartzlander, G. *Opt. Lett.* **1996**, *21*, 827–829.
- [32] Kuga, T.; Torii, Y.; Shiokawa, N.; Hirano, T. *Phys. Rev. Lett.* **1997**, *78*, 4713–4716.
- [33] Mei, Z.; Zhao, D. *J. Opt. Soc. Am. A*: **2008**, *25*, 537–542.
- [34] Cai, Y.; He, S. *Opt. Express* **2006**, *14*, 1353–1367.
- [35] Mei, Z.; Zhao, D. *J. Opt. Soc. Am. A*: **2005**, *22*, 1898–1902.
- [36] Eyyuboğlu, H.T. *Opt. Laser Technol.* **2008**, *40*, 156–166.
- [37] Lü, X.; Cai, Y. *Phys. Lett. A* **2007**, *369*, 157–166.
- [38] Sun, Q.; Zhou, K.; Fang, G.; Zhang, G.; Liu, Z.; Liu, S. *Opt. Express* **2012**, *20*, 9682–9691.
- [39] Lin, J.; Ma, Y.; Jin, P.; Davies, G.; Tan, J. *Opt. Express* **2013**, *21*, 13193–13198.
- [40] Love, G.D. *Appl. Opt.* **1997**, *36*, 1517–1524.
- [41] Weiner, A.M. *Rev. Sci. Instrum.* **2000**, *71*, 1929–1959.
- [42] Yang, Y.; Dong, Y.; Zhao, C.; Cai, Y. *Opt. Lett.* **2013**, *38*, 5418–5421.
- [43] Richards, B.; Wolf, E. *Proc. R. Soc. London, Ser. A* **1959**, *253*, 358–379.
- [44] Zhang, Y.; Ding, B. *Opt. Express* **2009**, *17*, 22235–22239.
- [45] Harada, Y.; Asakura, T. *Opt. Commun.* **1996**, *124*, 529–541.
- [46] Zhang, Y.; Suyama, T.; Ding, B. *Opt. Lett.* **2010**, *35*, 1281–1283.